TITLE OF MY THESIS

by

Student Name

A dissertation submitted in partial fulfillment of the requirements for the degree of

DOCTOR OF PHILOSOPHY
in
ELECTRICAL AND COMPUTER ENGINEERING

UNIVERSITY OF PUERTO RICO
MAYAGÜEZ CAMPUS
2024

Approved by:

_____	_____
Juana del Pueblo, Ph.D. President, Graduate Committee	Date
_____	_____
Juan Pueblo, M.S. Member, Graduate Committee	Date
_____	_____
Juan Pueblo, Ph.D. Member, Graduate Committee	Date
_____	_____
Juana Pueblo, M.S. Member, Graduate Committee	Date
_____	
Representative of Graduate Studies	_____
	Date
_____	
Juana del Pueblo, Ph.D. Chairperson of the Department	_____
	Date

ABSTRACT

This template was done to help you ease your work of redacting your thesis. It has easy tools such as adding an equation (with **Copy/Paste**) and it automatically updates the equation numbers not just next to the equation but also whenever it is reference. The same goes for **Figure** numbers within captions and within paragraphs. It can save you a lot of time and helps you have a more professional thesis with least amount of mistakes.

The template also shows you how to have *Table of Contents* updated in a second! (with a mere ***Right-click*** and ***Update fields***>*Update Entire Table and/or Numbers Only*) This is particularly important the last few days before deadline for submitting your thesis after applying changes suggested by your committee members.

The same goes for equations. To enter a new equation, or Figure/Table caption, copy any one already in the document and paste it. Then edit the equation. The **equation/ figure/ Table** number when updated, will have the correct chapter number and the correct equation/fig/table number. To refer or mention a particular figure in your text, do **Insert**>**Cross-Reference** and on "*Reference Type"*: choose **Figure**, **Table**, or **Equation**. Then on "*Insert Reference to*:" chose **only Label and Number**.

To update ALL fields within the document do ***Control-A***(or ***Command-A*** for **mac**), then **Right-Click** and **Update**.

RESUMEN

El resumen debe ser la traducción exacta del *Abstract*. Select this section with the mouse, and choose **Tools**>**Language**> **Spanish**> for this section only.

Make sure that each one of them, Abstract and Resumen, are only 1-page long each.

Bla blab la abla abla abal abla,

Bla abla abla

Bla bla abla abla

ACKNOWLEDGEMENTS

Blabla bla abla abla abla

TABLE OF CONTENTS

1 CHAPTER –INTRODUCTION....1

2 CHAPTER- LITERATURE REVIEW....3

1.1 STOCHASTIC MODELING AND SHORT-TERM RAINFALL FORECASTING....3
1.2 RADAR RAINFALL ESTIMATION AND VALIDATION....7

3 CHAPTER – METHODOLOGY....1

1.3 STUDY AREA....2
1.4 HIGH RESOLUTION RAINFALL RADAR PRODUCT....4
1.5 TROPINET RADARS....6
3.1.1 Radar Data Processing TropiNet....8
3.1.2 Calibration Performance....8
1.6 INUNDATION MODEL....8
3.1.3 Precipitation Estimation....10
3.1.4 Variables Initials and optimization....12
3.1.4.1 Least Square Method....15
3.1.4.2 Kriging Interpolation....15
3.1.5 Events selection....17
1.7 HYDROLOGIC MODEL COMPOSITION....18

4 CHAPTER - RESULTS....1

1.8 DATA ACQUISITION....1
1.9 RAIN GAUGES-TROPINET – NEXRAD COMPARISON....2
1.10 NOWCASTING MODEL MOVEMENT AND REFLECTIVITY ANALYSIS....5
1.11 PARAMETERS ESTIMATION....6

5 CHAPTER - CONCLUSION....10

REFERENCES....11

LIST OF TABLES

Table 3-1. Radar bands with frequencies and wavelength [*Rinehart*, 1997]).....6
Table 3-2. Characteristics of Studied Storm.....18
Table 3-3. Drainage area peak discharge relationship [FEMA, 2012].....19
Table 4-4. Detection results for ten storms with lead-time of 10 minutes.....8
Table 4-5. Detection results for ten storms with lead-time of 20 minutes.....8

LIST OF FIGURES

Figure 2-1. Flowchart Stochastic Model based [*Box and Jenkins*, 1976].....4
Figure 2-2. Forecast 1h and 2h ahead of hourly rainfall intensity and accumulative rainfall using event-based approaches for the event of 18 February 1953, Denver station, Colorado, USA [*Burlando et al*., 1993].....5
Figure 2-3. Long range problem with NEXRAD (based on *Cruz-Pol et al.*, 2011). The figure does not include topography of the land surface.....9
Figure 3-4. Digital Elevation Model.....3
Figure 3-5.TropiNet-2 at Lajas.....5
Figure 4-6. Comparison TropiNet and NEXRAD on May 06, 2014- 17:42.....3
Figure 4-7 . Comparison Rain Gauge-NEXRAD-Average.....4
Figure 4-8. Phi median, storm date: March 28, 2012, lead-time of 20 min.....7
Figure 4-9. Distribution of initial value of phi (left) and the optimal values of phi (right) for the storm date: March 28, 2012,for a lead-time of 30 min.....7

GLOSSARY OF TERMS

A	flow area
a, b	coefficients in the radar rain rate equation
AMS	Annual Maximum Series
ArcGIS	Arc Geographical Information Systems
ASCII	data file in text format
Bias	bias
C	Celsius
CASA	Collaborative Adaptive Sensing of the Atmosphere
DB	discrete bias
dBZ	decibels
DEM	digital elevation map
DHSVM	Distributed Hydrology Soils and Vegetation Model
e_a	actual vapor pressure
e_s	saturated vapor pressure
ET	evapotranspiration
ET_o	reference evapotranspiration
HEC	Hydrologic Engineering Center
HEC-RAS	Hydrologic Engineering Center-River Analysis System
kPa	kilopascal
NAD	North American Datum
N1P	precipitation radar product
NEXRAD	Next Generation Radar
Ni	adjustment factor
NOAA	National Oceanic and Atmospheric Administration
O	model output with input parameters set at base values
$O_{P+\Delta P}$ and $O_{P-\Delta P}$	are model outputs with the input parameter plus or minus a specified Percentage
R^2	Pearson correlation coefficient or coefficient of determination
R_a	extraterrestrial radiation
RMSE	root mean squared error
SSURGO	refers to the Soil Survey Geographic Database |
STD	standard deviation
t	time
TARS	Tropical Agriculture Research Station
T_{ave}	average air temperature
TBSW	Testbed Subwatershed
TM	Thermatic Mapper
T_{max}	maximum air temperature
T_{min}	minimum air temperature
TRMM	Tropical Rainfall Measuring Mission

1 CHAPTER –INTRODUCTION

Portions of Puerto Rico Western area are subject to flash flooding due to sudden, extreme rainfall events, some of which fail to be detected by NEXRAD radar located 104 km away in the town of Cayey, Puerto Rico and partially obstructed by topographic features. The use of new radars with higher spatial resolution and covering areas missed by the NEXRAD radar, are important for flood forecasting efforts, and for studying and predicting atmospheric phenomena.

Recently, the University of Puerto Rico in Mayagüez Campus, *Trabal et al*., [2011] initiated investigations using two (2) types of radars, namely: Off-the Grid (OTG) and TropiNet, with radius of coverage of 15 km and 40 km, respectively. This network will monitor the lower atmosphere where the principal atmospheric phenomena occur. This work represents the first time that TropiNet radar technology will be used for hydrologic analyses and specifically for rainfall forecasting in Puerto Rico western area.

Short-term rainfall forecasts have commonly been made using Quantitative Precipitation Forecast (QPF). The introduction of quantitative precipitation forecasting (QPF) in flood warning systems has been recognized to play a fundamental role, QPF is not an easy task, rainfall being one of the most difficult elements of the hydrological cycle to forecast [*French et al*., 1992] and great uncertainties still affect the performances of stochastic and deterministic rainfall prediction models [*Toth et al.,* 2000].

This capability currently does not exist in Puerto Rico Western area, and is needed because of the potential for flooding in certain areas (e.g., in flood plains near the principal rivers). In this research, short-term rainfall forecast analysis performed using non linear stochastic methods. Once obtained, the rainfall forecast is introduced into a hydrologic/inundation model *Vflo* and Inundation Animator configured for the *Vflo* Bay Drainage Basin (MBDB).

Specific components of the research are: the inclusion of calibration and validation of rainfall estimates produced by the TropiNet radar network, the development and validation of the stochastic rainfall prediction methodology, the calibration and validation of the inundation algorithm at selected locations within the MBDB, and the proto-type of an operational, real-time flood alarm system for the MBDB. The proto-type, automated flood alarm system will send near-real time updated inundation images to a website on the Internet.

This research consists of a review of the scientific literature in Chapter 2, justification for the research in Chapter 3, objectives in Chapter 4, and the methodologies for the research are given in Chapter 5. The results are provided in Chapter 6.

2 CHAPTER- LITERATURE REVIEW

In this section we will provide a brief review of the literature related to each of the components of the proposed project. These components include: stochastic modeling and short-term rainfall forecasting, radar rainfall estimation and validation, hydrologic/inundation modeling and real-time flood forecast systems.

1.1 Stochastic Modeling and Short-Term Rainfall Forecasting

There are many approaches that can be used to predict the future direction and magnitude of a physical process, such as rainfall. Forecasting is a large and varied field having two predominant branches: Qualitative Forecasting and Quantitative Forecasting [*Hyndman*, 2010]. Quantitative Forecasting should satisfy two conditions, the accessible numerical information about the past and assumptions that some aspects of the past patterns will continue into the future. Quantitative Forecast can be divided into two classes: time series and explanatory models. Explanatory models assume that the variables to be forecast exhibits an explanatory relationship with one or more other variables, in contrast, time series forecasting uses only information on the variable to be forecast, and makes no attempt to discover the factors affecting its behavior [*Hyndman*, 2010]. The time series models attempt to capture past trends and extrapolate them into the future. There are many different time series models but the basic procedure is the same for all as illustrated in Figure 2 -1.

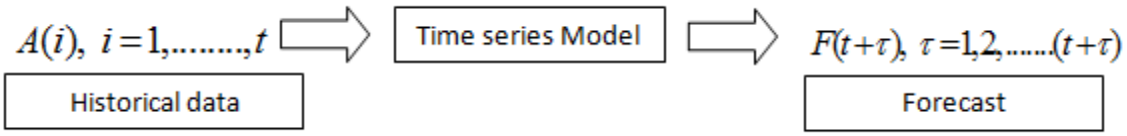

Figure 2-1. Flowchart Stochastic Model based [*Box and Jenkins*, 1976]

Some of the most common time series methods include: Autoregressive, Moving Average, Exponential Smoothing, Autoregressive Moving Average, Extrapolation, Linear Prediction and others [*Box and Jenkins*, 1976], this research include a new type of time series non linear with a stochastic and deterministic components, this will be explained later.

The autoregressive (AR) method is a type of random process, which is used to predict some types of natural phenomena, falling within the group of linear prediction formulas. The moving average (MA) method is a way to convert actual observations to forecast by simply averaging [*Box and Jenkins*, 1976]. Exponential smoothing is a popular scheme to produce a smoothed time series; exponential smoothing assigns exponentially decreasing weights to the observations as they get older. That is to say recent observations are given relatively more weight in forecasting than the older observations. With the Autoregressive Moving Average (ARMA) method, models are used to describe stationary time series, which represent the combination of an autoregressive (AR) model and moving average (MA) model. The order of the ARMA model in discrete time (t) is described by two integers (p, q), that are the orders of the AR and MA parts, respectively. A process is considered to be stationary when parameters, such as the mean and variance, do not change over time or maintain the same range. Autoregressive (AR) or

Autoregressive moving average (ARMA) are models widely used in the prediction. Other time series methods include extrapolation and linear prediction, non linear prediction with exponential component, depending of data behavior.

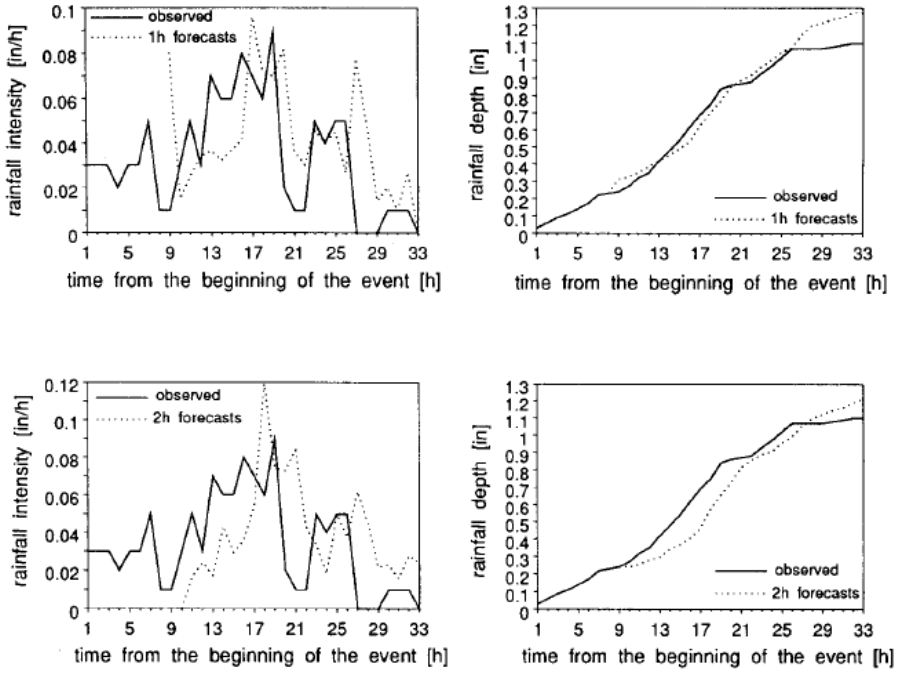

Figure 2-2. Forecast 1h and 2h ahead of hourly rainfall intensity and accumulative rainfall using event-based approaches for the event of 18 February 1953, Denver station, Colorado, USA [*Burlando et al*., 1993].

Burlando et al., [1993] assumed that the rainfall processes are typically non-stationary and skewed. To circumvent non-stationary, the rainfall data are grouped by month of season; thus the model is applied separately for data of a given month or a given season. Accordingly, model parameters such as autoregressive and moving average coefficients were determined from precipitation data pertaining to a given month or season only.

Parameter estimation of ARMA models based on short-term precipitation records defined at hourly time-scales is more complex than when data is defined at longer time periods such as months. The main reason is the intermittent characteristic of hourly precipitation. A popular decision rule for comparing models in the time series literature is the Akaike Information Criterion (AIC) [*Akaike*, 1974]. This criterion is known as the test for the
The maximum likelihood estimation criterion is suited for the selection of a model for simulation purpose. For short-term forecasting, such as one step ahead forecasting, the mean square error (MSE) criterion may be more useful [*Kashyap and Rao*, 1976].

Selection of a model based on an MSE criterion is quite simple and can be summarized as follows:

1. Estimate the parameters of different models using a portion, usually half of the available data.
2. Forecast the second half of the series one step ahead by using the candidate models.
3. Estimate the MSE corresponding to each model and
4. Select the model that results in the least value of the MSE.

Other examples of rainfall forecasting models were developed. PRAISE (Prediction of Rainfall Amount Inside Storm Events) is a stochastic model to forecast rainfall height at site. PRAISE is based on the assumption that the rainfall height accumulated on a delta time is correlated with a variable that representing antecedent precipitation. The mathematical background is given by a joined probability density function and by a bivariate probability distribution, referred to the random variable, represents rainfall in a

generic site and antecedent precipitation in the same site. The peculiarity of PRAISE is the availability of the probabilistic distribution of rainfall heights for the forecasting hours, conditioned by the values of observed precipitation. PRAISE was applied to all the telemetering rain gauges of the Calabria region, in Southern Italy; the calibration model shows that the hourly rainfall series present a constant value of memory equal to 8 hours, for every rain gauge of the Calabria network. As a study area the Calabria region in southern Italy was selected to test performances of the PRAISE model [*Sirangelo et al.,* 2007].

1.2 Radar Rainfall Estimation and Validation

The National Weather Service is in charge of providing weather, hydrology, and climate forecasts and warnings for the United States including Puerto Rico and U.S Virgin islands, working with a network of 159 high resolutions Doppler weather radars, commonly referred to as NEXRAD (NEXRAD or Next-Generation Radar). The technical name for NEXRAD is WSR-88D, which stands for Weather Surveillance Radar, 1988, Doppler (National Climatic Data Center, 2012). NEXRAD detects precipitation and atmospheric movement or wind. The NEXRAD radars can provide information that can help mitigate disasters caused by flash floods. Errors can occur with the methodology for observations far from the radar, where the earth's curvature limits the observation of the lower atmosphere, see Figure 2 -3. NEXRAD coverage has limitations in observing below 10,000 feet or 3 kilometers (called the Gap) above sea level for the Mayagüez area

and nearby towns [*Cruz-Pol et al.,* 2011]. At these locations, NEXRAD cannot "see" if raindrops are forming within the Gap, resulting in a different rain rate than other radars which can measure the lower portion of the cloud (OTG and TropiNet). In the OTG and TropiNet radars, the rain rate equations can be selected, whereas NEXRAD rain rate uses the tropical equation with a threshold reflectivity (Z) of 53dBz, Z values above 53 dBz are assumed to be hail and are not considered. Other difference between NEXRAD and TropiNet radar is that NEXRAD has Doppler capabilities given information on cloud motion, and TropiNet has Polarimetric capabilities which give information on precipitation type and rate. Polarimetric radars refer to dual polarization radars which transmit waves that have horizontal and vertical orientations. The horizontal wave provides a measure of horizontal dimension of the cloud and rainfall and the vertical wave provides a measure of particle size, shape and density.

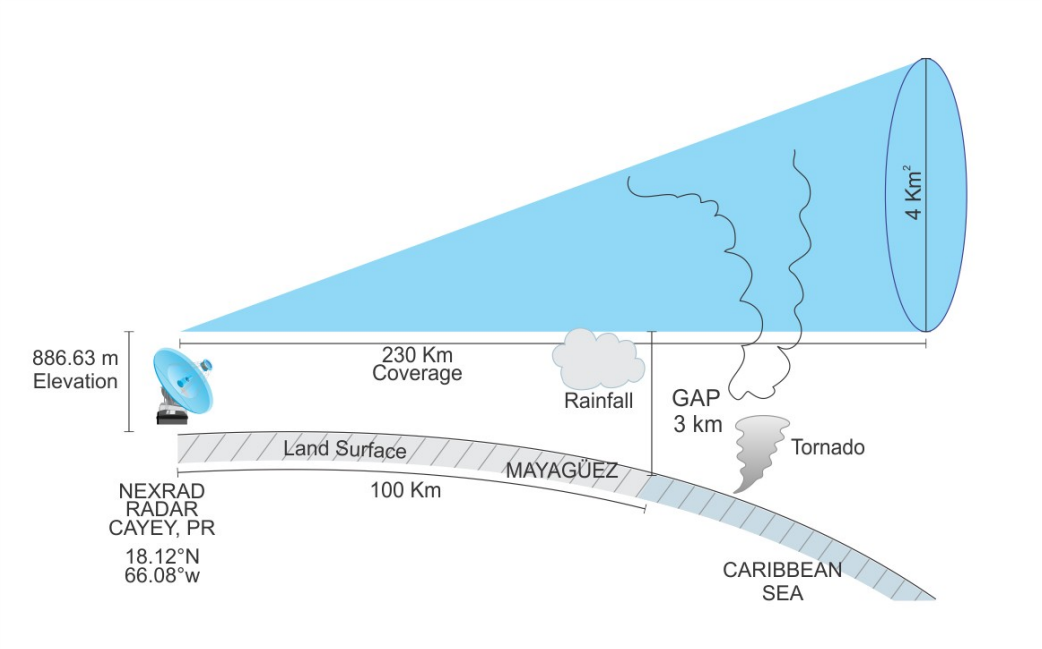

Figure 2-3. Long range problem with NEXRAD (based on *Cruz-Pol et al.*, 2011). The figure does not include topography of the land surface.

The use of the new radars OTG and TropiNet with higher spatial resolution and their observations of the lower atmosphere in the Western Puerto Rico area provide better atmospheric information in the lower zone because curvature effect is minimal, at minimum elevation.

3 CHAPTER – METHODOLOGY

The University of Puerto Rico at Mayagüez has a radar research network and a rain gauge network developed for this thesis. The radars network provide information with higher spatial and temporal precision, TropiNet has resolution spatial of 60x60 meter every pixel and temporal resolution of 1 minute. A flood warning model must be operated based only on the data available at the time of forecast. Only the radar can display data in real time, this is not possible using rain gauges. Rain gauges based systems must have a dependable and redundant telemetry system that will accurately and efficiently transmit data a central location for processing.

The Data from TropiNet radar was used for rainfall prediction in MBDB, using stochastic methods. Once the rainfall forecast is obtained, the use of hydrologic models is necessary for analysis of flooding in this area.

This chapter present a general overview of the methodology utilized in this investigation, this is the first attempt to implement news technology to the performance of flood alert/warning systems. This research is center in the Puerto Rico western area and could be applied in general to other areas or regions with the same rainfall type.

1.3 Study Area

The study area, which encompasses the MBDB, is 819.1 km^2 in area [*Rojas*, 2012 and *Prieto*, 2007] and is located in western Puerto Rico. The watershed also has three (3) important water bodies: Rio Grande de Añasco, Río Guanajibo and Río Yagüez. The area includes twelve (12) municipalities: Mayagüez , Añasco, Las Marías, San Sebastián, Lares, Maricao, Yauco, Adjuntas, Sabana Grande, San Germán, Hormigueros and a part of Cabo Rojo.

The Río Grande de Añasco originates near the Cordillera Central, flows west and discharges into the Bahia de Añasco, the alluvial valley covers an area of approximately 46.62 km^2. It is bounded by hills to the north, east and south and by the Bahia de Añasco to the west. The tributaries of the river Añasco that flow into the lower valley are the Rio Dagüey and the Rio Cañas. The basin is located in west-central Puerto Rico, in the municipalities of Añasco, Lares, Las Marias, Maricao, Mayagüez and San Sebastián. Changes in elevation are shown and vary from zero meters at mean sea level in the coastal areas to 960 meters in the mountainous areas, see Figure 3 -4. According to U.S Environmental Protection Agency, the upper reaches of the basin contain four connected reservoirs; the lago Toro, Lago Prieto, Lago Guayo and Lago Yahuecas, to the Añasco watershed downstream of the lakes which is not significant for regional water budget estimation [*Prieto*, 2007]. The total lake drainage area is about 116.55 km^2 and was used as a boundary condition in the model.

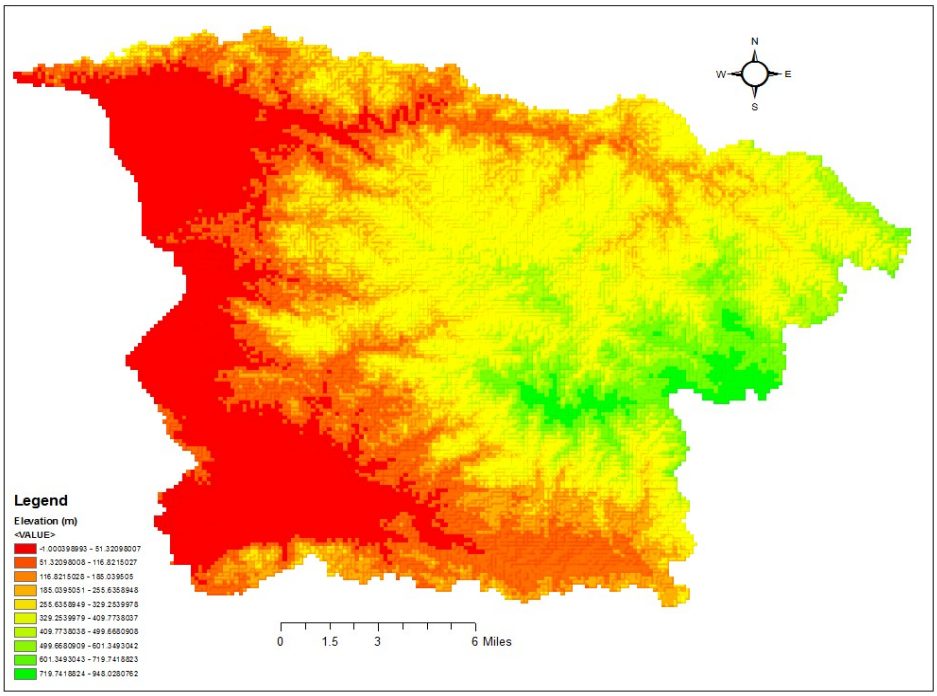

Figure 3-4. Digital Elevation Model.

According to Flood Insurance Study by Federal Emergency Management Agency [FEMA, 2012] the land use on the Río Grande de Añasco watershed are distributed as follows: 278 km^2 are cropland; 114 km^2 are pasture; 85km^2 are forest and woodland; 33 km^2 are idle, and 13 km^2 are urban development and other uses. The vegetation in the floodplain is primary sugar cane. Soils in the floodplain are clay loams (Unpublished Soil Borings in Añasco Basin).

Flood problems in this study area are serious and widespread. Periodic flood damage to sugar cane, pastureland, roads, and a number of residential areas is significant. Flood

waters have inundated the main Río Grande de Añasco floodplain 17 times in a period of 31 years, an average of approximately once every 2 years.

1.4 High Resolution Rainfall Radar Product

Commonly, the flood alert systems have fulfilled the role of providing flood notification to many people and have saved lives and properties. However, many alert systems fail due to low precision of the models and the sudden change of the atmosphere. One of the greatest sources of uncertainties in the prediction of flooding is the rainfall input [*Rojas*, 2012]. It is therefore essential to have an accurate source of rainfall data, and this is only possible with properly working radars.

The National Weather Service has a network of 160 Doppler-radar stations S-band (10-cm wavelength) radar distributed across the continental United States, Alaska, Hawaii, Guam and Puerto Rico. This network was originally designed to support Departments of Defense, Transportation and Commerce objectives for detection and mitigation of severe weather events [*Warner et al*. 2000]. Digital distributed-precipitation radar products can be downloaded directly from the National Weather Service (NWS).

The NEXRAD (Next-Generation-Radar) located in Cayey measures reflectivity to 1 km by 1 degree resolution to a diameter (distance) of 460-km.

Figure 3 -5 shows the TropiNet radar at Lajas. A new TropiNet radar is being installed at the UPR Agricultural Experiment Station in Isabela, which has the same characteristics as the other two. When the three TropiNet radars are operating simultaneously the cover area will be approximately half of the island.

Figure 3-5. TropiNet-2 at Lajas.

The OTG radars were developed with a heterogeneous network using off the shelf hardware. The network was designed to provide detailed precipitation estimates (QPE) to the public, including the (NWS) National Weather Service staff in Puerto Rico. Coincidentally, on the opening day of the Central American Games “Mayagüez 2010”, NEXRAD was offline and missed a large rainfall event which occurred in the Mayagüez area, but the “Weather Radar Network of Puerto Rico” radars were functioning and were able to record the event.

1.5 TropiNet radars

Radars are an active sensor that emits electromagnetic pulses into the surroundings. A typical radar system consists of a least four components: [*Rinehart*, 1997]. Lower frequency and higher wavelength suggest that the radar has robust signal power and less attenuation, the weather radar system discussed in this thesis is based in X-band. The common weather radar system can be classified as listed in Table 3 -1.

Table 3-1. Radar bands with frequencies and wavelength [*Rinehart*, 1997])

Radar Band	Frequency	Wavelength
L	1-2 GHz	30-15 cm
S	2-4 GHz	15-8 cm
C	4-8 GHz	8-4 cm
X	8-2 GHz	4-2.5 cm
K_U	12-18 GHz	2.5-1.7 cm
K	18-27 GHz	1.7-1.2 cm
K_a	27-40 GHz	1.2-0.75 cm
W	40-300 GHz	0.75-0.01 cm

The TropiNet (RXM-25) radars are Doppler polarimetric radars which allow the radar beam to measure reflectivity close to the ground, overcoming the shadow effect of the Earth's curvature, while maintaining high range and azimuth. The first of three proposed radars has been developed and it is in operation since February 2012, TropiNet 1 is located in "Cerro Cornelia" Cabo Rojo, Puerto Rico 18.16°N, 67.17°W, and 200 ft elevation (msl) approximately. The radars, working with the X-band frequency, are about

three times stronger than that of the traditional radar frequencies at S-band making the measurements of rainfall more attractive. They have high space and time resolution for weather monitoring and detection, and are capable of generating very high resolution data with a range of 40 km or maximum radial distance (horizontal range) of 80 km.

NOAA-NWS [1995] report recommended that *Z-R* relationship in use at the time of the event be changed from $Z = 300R^{1.4}$ to a relationship more representative of raindrop distributions in a warm tropical storm. The Z-R relationship for warm tropical events recommended by OSF since 1995 for all WSR-88D sites experiencing heavy rainfalls, and now adopted by TropiNet is $Z = 250R^{1.2}$. The *Z-R* relationship used in Puerto Rico is the convective, also was necessary to define a maximum precipitation rate threshold for decibels above 53 dBz [*Vieux and Bedient*, 1998]. The convective rainfall is a type of precipitation with some characteristics like very high horizontal gradient and very large vertical depths, these characteristics means that the weather radar is the best tool for detecting convective precipitation, but the presence of different types of hydrometeors, especially hail and storm dynamics resulting in fast varying Vertical Profile Reflectivity (VPR) usually result in considerable random error in quantitative precipitation estimates. Large differences can be found especially when comparing rain gauges and radar estimates because of the high temporal and spatial variability of the convective storm and related vertical profile of reflectivity [*Rossa et al.*, 2005].

3.1.1 Radar Data Processing TropiNet

A radar application in MatLab was developed to access the store of binary volume files that contain the respective information as determined by the operator like reflectivity, azimuth, velocity, beam width, range, elevation and other radar products. The operator can apply any possible scan forms Range Height Indicator (RHI).

3.1.2 Calibration Performance

There is a sequence called the “Ordered Physics Based Parameters Adjustment” (OPPA) method developed by *Vieux and Moreda* [2003]. The calibration process (OPPA) approach include estimates of the spatially distributed parameters from physical properties, assigns channel hydraulic properties based on measured cross-sections where available, studies model sensitivity for the particular watershed, and identifies response sensitivity to each parameter.

1.6 Inundation Model

The Inundation Analyst is a *Vflo* [*Vieux et al.,* 2002] extension that provides images, animations and simulated inundation, which is an indication of flood risk. The extension is especially useful for flood management applications; for example, a forecast inundation is useful for operational decisions, warning and notification, and coordinating

emergency response. The Inundation Analyst operates independently from the *Vflo* model, but can use data exported from *Vflo* as input for generating inundation forecasts. The Inundation Analyst requires a digital elevation model (DEM), a flow direction map, a channel flow direction map, and stage data. All input data must be in ESRI ASCII grid format (*.*asc*).

All input data are ASCII and the flow direction is extracted from the DEM watershed. The DEM have units of meters, the stage data input are exported from *Vflo* model, a background watershed image is included in bitmap format. The inundation results are listed in order to create the animation, once all stage files are listed in the appropriate order the images that are produced show the primary inundation Analyst window.

$$di = \sqrt[2]{\left(x_{ti} - x_{ti-1}\right)^2 + \left(y_{ti} - y_{ti-1}\right)^2} = \sqrt[2]{\Delta x^2 + \Delta y^2}\,(km) \tag{3-1}$$

$$\theta = \tan^{-1}\frac{\Delta y}{\Delta x}(rad) \tag{3-2}$$

$$v = \frac{d(km)}{t(min)} \tag{3-3}$$

To determine the centroid of the cells it is necessary to calculate latitude $(\overline{La})$ and longitude $(\overline{Lon})$ of every pixel group.

$$\overline{La} = \frac{1}{n}\sum_{i=1}^{n} la_i \tag{3-4}$$

$$\overline{Lon} = \frac{1}{n}\sum_{i=1}^{n} lo_i \qquad (3\text{-}5)$$

Dixon and Wiener [1993] found that a convective cell have a mean velocity of 64km/hr, this value agrees with the velocity cell measure from other research, for this model a velocity mean of 72 km/hr approximately or 12km/10minutes was used, to apply this a maximum distance between cloud at every lag time of 200 pixels was necessary, if the analysis is every 10 minutes, if this analysis time increase, then the distance could increase.

3.1.3 Precipitation Estimation

The precipitation estimation is based in the main equation applied to each zone in every window. The rain estimated $\hat{h}_{t+1,k(i,j)}$ at time ($t+1$¿, is the result of the prediction interval $\Delta t(10,20,30)$ between the instants $i\Delta t$ and $(i+1)\Delta t$ correlated with the variables $(\alpha,\beta,\Phi,\delta 1,\delta 2,\delta 3)$ that are change in the 8,528 zones, these variables were determined in each zone (9x9) using optimization techniques for nonlinear regression. The main equation includes three (3) fundamental products: $\overline{h}_{t-1,k(i,j)}, \overline{h}_{t-2,k(i,j)}, h_{t-1,k(i,j)} \wedge Z_{t-1,k(i,j)}$ these are the average observed rain at time $t-1$ and time $t-2$, the average is calculated

between the eight (8) nearest pixel to the prediction pixel, the other $h_{t-1,k(i,j)}$ is the value of the rain at $(t-1)$, and the $Z_{t-1,k(i,j)}$ is the ratio of reflectivity at $(t-1)$.

The main equation has some restrictions in the variables $(\alpha,\beta,\Phi,\delta 1,\delta 2,\delta 3)$ that are changing in time and space. The clouds are in movement and the values of the variables are changing continuously. After the optimization, the deltas values are restricted to be positive or equal to zero.

$$\delta_{i,t,k} \geq 0 ; i = 1,2,3 \tag{3-6}$$

The variables of α,β are the minimum and maximum reflectivity value respectively between the last two (2) windows at $(t-1)$ and $(t-2)$at the zone (9x9), these variables are changing in time and space (every zone 9x9). Moreover the variable $\Phi_{t,k}$ changes in every zone and windows but having a restriction limit of 1.1 in the optimization routine.

$$\alpha = min\left(Z_{t-1}, Z_{t-2}\right) \tag{3-7}$$

$$\beta = max\left(Z_{t-1}, Z_{t-2}\right) \tag{3-8}$$

$$0 < \Phi_{t,k} \leq 1.1 \tag{3-9}$$

Once the variables were found the next step was to estimate the rain rate forecast in every pixel. Pixels that were not possible to do the estimation prediction or there is not enough

data at time $t-1$ and/or at time $t-2$, the "*Kriging*" interpolation method was used to estimate the rain pixel to derive the corresponding predictors [*Wackernagel*, 2003].

3.1.4 Variables Initials and optimization

The variables into the nonlinear equation model are fundamental in the precipitation forecast trend. A well-planned approach is needed to properly solve the nonlinear constrained problem. The explored approach includes two steps: (i) Identifying the initial point and (ii) Using a constrained nonlinear optimization technique to estimate the final parameter set for each zone and every window.

To estimate the initial values of deltas, it was not necessary to apply a constrain, so that the initial deltas values can be positives or negatives. The main equation was linearized taking known values of $h_{t,k(i,j)}, \overline{h}_{t-1,k(i,j)}, \overline{h}_{t-2,k(i,j)}, \alpha_{t,k}, \beta_{t,k}$ and $Z_{t-1,k(i,j)}$ and the unknown values of $\delta 1_{t,k}, \delta 2_{t,k}, \delta 3_{t,k}$, left the parameter phi $\Phi_{t,k}$ temporarily ignored.

This method consists in solving the equivalent linear model and using these values as the initial point. The convergence of nonlinear routine heavily depends on the selections of the initial points. Thus, if the initial point is far away from the optimal solutions the algorithm may converge to a suboptimal point or may not converge.

Linearizing and ignoring the phi variable:

$$-\ln\left[1-\left(\frac{h_{t,k(i,j)}-\alpha_{t,k}}{\beta_{t,k}-\alpha_{t,k}}\right)\right]=\sum\left(\delta 1_{t,k}\bar{h}_{t-1,k|i,j|}+\delta 2_{t,k}\bar{h}_{t-2,k|i,j|}+\delta 3_{t,k}Z_{t-1,k|i,j|}\right)+ \quad (3\text{-}10)$$

where

$$\beta_{t,k}>h_{t,k|i,j|}\wedge\alpha_{t,k}<h_{t,k(i,j)} \quad (3\text{-}11)$$

$\varepsilon_{t,k|i,j|}$ is an unknown random variable at time *t* and at location (i,j) of the *k* zone, the initial values of delta are obtained by solving the linear regression by the least square method.

The phi parameter is a bias correction factor and can be estimated using a second linear regression.

$$\left[\frac{h_{t,k|i,j|}-\alpha_{t,k}}{\beta_{t,k}-\alpha_{t,k}}\right]=\Phi_{t,k}¿¿ \quad (3\text{-}12)$$

$$+\varepsilon_{t,k|i,j|}$$

where the condition in the Equation (3 -11) is present $\beta_{t,k}>h_{t,k|i,j|}\wedge\alpha_{t,k}<h_{t,k(i,j)}$

$\varepsilon_{t,k|i,j|}$ is an unknown random variable at time *t* and at location (i,j) in the zone 9x9.

Simplifying with the initial delta estimates the following equation is obtained.

$$\lambda_{t,k(i,j)}=\Phi_{t,k}\left(\theta_{t,k|i,j|}\right)+\eta_{t,k(i,j)} \quad (3\text{-}13)$$

where

$$\lambda_{t,k(i,j)}=\frac{h_{t,k(i,j)}-\alpha_{t,k}}{\beta_{t,k}-\alpha_{t,k}} \tag{3-14}$$

$$\theta_{t,k(i,j)}=¿¿ \tag{3-15}$$

$\eta_{t,k(i,j)}$ is an unknown random variable at time t and at location (i,j) of the k zone, $\hat{\delta}$'s are the previous estimated or initial values of deltas.

The next step is the most important in this section, finding the optimum values of variables $\delta 1_{t,k},\delta 2_{t,k},\delta 3_{t,k}$ and$\Phi_{t,k}$ from initial values determined in the previous steps. The parameters of the nonlinear regression model can be easily estimated by solving a constrained nonlinear optimization problem.

$$\delta i_{t,k}\geq 0; i=1,2,3 \tag{3-16}$$

$$0<\Phi_{t,k}\leq 1.1 \tag{3-17}$$

Therefore, it can be solved by using the "*sequential quadratic programming"* algorithm [*Reklaitis et al.*, 1983; MathWorks, 2011]. The derived initial point was ingested into the constrained nonlinear subroutine to facilitate convergence, the parameters of the exponential term were restricted to be positive, and the phi parameter was restricted to be in the range of 0 to 1.1 value, this threshold was derived by inspection. The optimization objective was minimizing the errors between the estimate values for the regression and the observed values by radar.

In these regions in the prediction where there are clouds (or cells) present in the movement estimation, but not the required minimum number of pixels, the pixels estimation predictions were obtained by *Kriging* interpolation.

3.1.4.1 Least Square Method

The least squares estimate of the multiples regression parameters were used to calculate the initial values of deltas variables. The multiple linear regression model is typically stated in the following form:

$$y_i = U_0 + U_1 x_{1j} + U_2 x_{2j} + \ldots + U_N x_{Nj} + \epsilon_j \qquad (3\text{-}18)$$

where the dependent variable is y_i, $U_0, U_1, U_2, \ldots, U_N$ are the regression coefficients and ϵ_j is the random error assuming $E(\epsilon_j) = 0$ and $Var(\epsilon_j) = \sigma^2$ for $j = 1, 2, \ldots, M$.

3.1.4.2 Kriging Interpolation

Kriging is based on the assumption that the parameter being interpolated can be treated as a regionalized variable. A regionalized variable is intermediate between a truly random variable and a completely deterministic variable in that it varies in a continuous manner

from one location to the next and therefore points that they are near each other and have a certain degree of spatial correlation, but points that are widely separated are statistically independent [*Davis*, 1986].

The *Kriging* techniques are based on the estimation of weighting coefficients with an assumption of unbiased-ness. Each data has its own coefficient *w*, which represent the influence of a particular data on the value of the final estimation at the select grid node. The relationship between the existing data and the estimation point has been expressed by variogram values or by covariance in case of second order stationarity. Such values describe the spatial dependence and the influence of the particular location in terms of its distance and direction from the estimated location [*Malvic and Balic*, 2009].

The basic equation used in ordinary *Kriging* is as follows:

$$F(x,y)=\sum_{i=1}^{n} w_i f_i \tag{3-19}$$

where n is the number of scatter points in the set, f_i are the values of the scatter points, and w_i are the weights assigned to each scatter point. The weights are found through the solution of the simultaneous equations:

$$\begin{aligned} w_1 S(d_{11}) + w_2 S(d_{12}) + w_3 S(d_{13}) &= S(d_{1p}) \\ w_1 S(d_{12}) + w_2 S(d_{22}) + w_3 S(d_{23}) &= S(d_{2p}) \\ w_1 S(d_{13}) + w_2 S(d_{23}) + w_3 S(d_{33}) &= S(d_{3p}) \end{aligned} \tag{3-20}$$

where $S(d_{ij})$ is the model variogram evaluated at a distance equal to the distance between points$i$ and j. It is necessary that the weights sum to unity.

$$w_1 + w_2 + w_3 = 1.0 \tag{3-21}$$

The *Kriging* techniques add some constraints to the matrices, to minimize the error, and these techniques are unbiased-ness estimations. These factors would describe some external limit on the input data, which cannot simply be observed in the measured values [*Malvic and Balic*, 2009].

3.1.5 Events selection

To select the events it was necessary to analyzed every one storm during 2012 and 2014, the analysis has three (3) important steps: the first was taking every minute data from TropiNet radar and plot it, for this was necessary create an efficient routine in MatLab to determine that the radar data has not interruptions or damage, if instead the radar has corrupt data the storm is discard to be evaluated. In some cases it was found that the radar takes data in “Plan Position Indicator’ (PPI) and after the radar is changed to “Range High Indicator” (RHI), such data was also discarded.

Table 3 -2 includes the dates and specifications of every storm to study, the information incorporate in the column “Storm Impact” was provided by National Weather Services (NWS) at Carolina, Puerto Rico (personal communication Carlos Ansemi).

Table 3-2. Characteristics of Studied Storm.

Date	Duration (UTC)	Storm Type	Storm Impacts
May 21, 2014	7 hr. 16:46-23:00	Heavy convective storm	The water covers the roadway. Ponding of water on roadways
June 29, 2014	5 hr. 17:00-22:00	Convective storm	The shower activity produced periods of moderate to locally downpours
June 30, 2014	4 hr. 16:00-20:15	Thunderstorms associated to the leading edge of a tropical wave	Moderate to heavy rain, urban and small stream flood advisory
July 05, 2014	4 hr. 16:44-20:00	Convective storm	Heavy rain, urban flood.

1.7 Hydrologic Model Composition

The hydrological Model used in this research was *Vflo*, this model use finite elements that can simulate streamflow based on geospatial data to simulate interior locations in the drainage network and determine channel flow and overland flow, it was fundamental a physical configuration of the watershed to be studied, such as a Digital Elevation Model (DEM), the topography digitalized, soils map, Land use map and information about the

basin. Some hydrologic and hydraulic studies have been conducted by *Sepulveda et al.*, [1996]; *Rojas* [2012].

Table 3-3. Drainage area peak discharge relationship [FEMA, 2012].

Drainage Area (sq km)	**Station Name**	**Peak Discharge (cms)**			
		10%	2 %	1 %	0.2 %
467.73	Rio Grande Añasco at Mouth	1,809	3,797	5,130	10,542
347.33	Rio Grande Añasco Near San Sebastian	1,390	3,031	4,078	8,329
385.26	Rio Grande Añasco upstream confluence Rio Casey	1,527	3,289	4,432	9,070
414.88	Rio Grande Añasco downstream confluence Rio Casey	1,631	3,481	4,695	9,624
35.4	Rio Yaguez at Mouth	292	595	770	1,289
329.65	Rio Guanajibo at Mouth	1,352	3,896	5,745	14,294
310.53	Rio Guanajibo Near Hormigueros	1,215	3,637	5,343	13,196
91.39	Rio Guanajibo at Hwy 119 at San German	604	1,325	1,713	2,991
303.04	Rio Guanajibo downstream confluence Rio Rosario	1,206	3,507	5,137	12,620

The following sections present the analysis of each variable in the hydrological model and determining the best parameters for a good operation. The analysis was based on existing literature within the study area.

4 CHAPTER - RESULTS

This chapter present the results of this research since obtaining, handling and processing data radar as well as the development of nowcasting model, validation of results, comparison between TropiNet radar and NEXRAD radar, configuration of hydrological model, implementations of nowcasting results and observed data into the hydrological model, configuration of inundation model, implementation of observed data and estimated data from hydrological model to inundation Analysis extension and finally comparison between USGS station and stations in the hydrological model.

1.8 Data Acquisition

Numerous storms were analyzed during 2012 and 2014 to select the suitable storms to be forecast, some requirements to choose the storm were necessaries: the data should be constant without interruptions, the radar should have the same elevation angle for all storms, the data may not be altered, and the radar should not stop during the storm or change its positions.

The TropiNet data was accessed from *weather.uprm.edu* server, the data is raw data in binary format. Two types of transformations from binary to net-cdf were needed to handle data and from net-cdf to mat, these transformations required the development of subroutines in MatLab. Other transformations necessary included changing the polar

coordinates to Cartesian coordinates; this was done to handle the data in the hydrological model *Vflo*.

1.9 Rain gauges-TropiNet – NEXRAD comparison

A routine was implemented to compare between Rain Gauges, TropiNet and NEXRAD data. The NEXRAD pixels have 1 square kilometer area and the TropiNet pixels have 60 meter for each side, this means that 256 TropiNet pixels equivalent in size to one (1) NEXRAD pixel or within one NEXRAD pixel fit 256 TropiNet pixels. Two comparison types were done, the first was pixel to pixel, and the second was average TropiNet pixels (256) with one NEXRAD pixel.

Figure 4 -6 presents a comparison image on a specific minute between TropiNet and NEXRAD, and shows the same storm but superimposed with the TropiNet image with the NEXRAD. This assignment was made for all storms analyzed to verify the storms location and confirm that the comparison data rain-rate is successful.

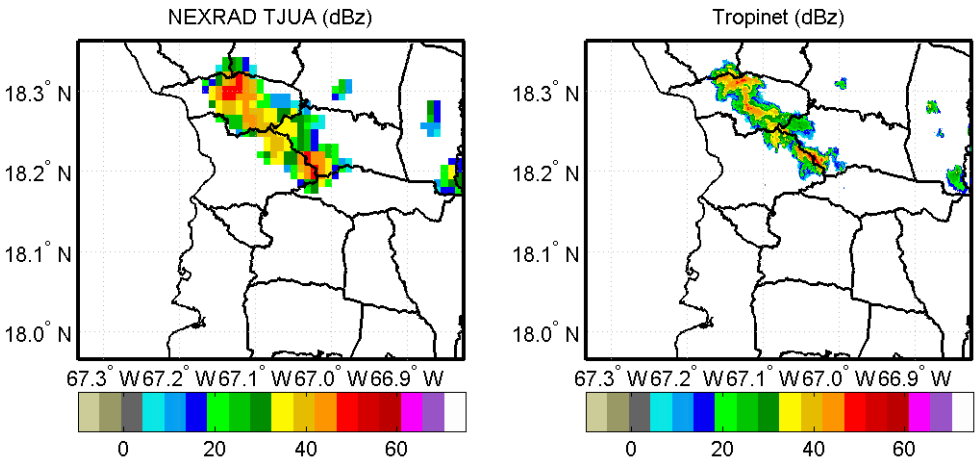

Figure 4-6. Comparison TropiNet and NEXRAD on May 06, 2014- 17:42.

Figure 4 -7 shows the comparison between NEXRAD and TropiNet at station C1, event May 21, 2014, the difference here is the average pixels (256) in TropiNet to change the resolution similar to NEXRAD.

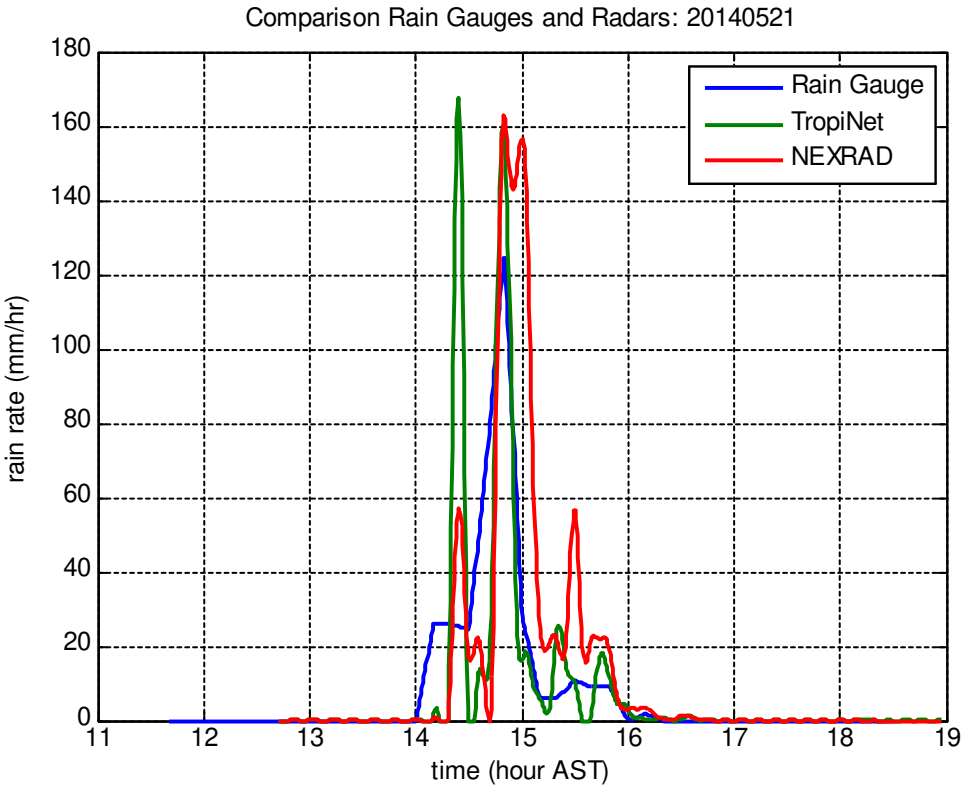

Figure 4-7 . Comparison Rain Gauge-NEXRAD-Average TropiNet –C1-May 21, 2014.

It includes the statistic results where MSE is the mean squared errors between Rain gauge-TropiNet and Rain gauges-NEXRAD and RMSE is the root means squared errors. The error is greater when the comparison between rain gauge and NEXRAD data is present, likewise the best result was observed between rain gauge and TropiNet data radar when it has the original resolution (60 meters).

$$SSE_T = \sum_{i=1}^{n} e_{N,i}^2 \qquad (4\text{-}1)$$

SSE is the sum-squared errors, the subscript T refers to TropiNet and subscript N refers to NEXRAD.

$$MSE_T = \frac{\sum_{i=1}^{n} e_{T,i}^2}{n} \tag{4-2}$$

$$MSE_N = \frac{\sum_{i=1}^{n} e_{N,i}^2}{n} \tag{4-3}$$

MSE is the mean square errors in TropiNet (T) and NEXRAD (N), and the next equation is the roots mean squared errors RMSE with the same subscript as the last equations.

Other comparisons were done with different dates between 2012 and 2014. Unfortunately, 20 (twenty) rain gauges were used and only few captured good data. In most rain gauges alterations were found to the equipment due to the natural or human factors.

1.10 Nowcasting Model Movement and Reflectivity Analysis

There are many methods to forecasting with long lead-time as: 8, 24, and 36 hours or weekly, using autoregressive methods, moving averages and others. This is a special kind of method to nowcasting (short time as minutes). In the Puerto Rico western area occur

sudden precipitations with short durations due to atmospheric conditions and locations, the precipitations take place immediately and its durations is around 1, 2 or 3 hours.

This shows the cloud motion comparison between observed (right) movement and estimated (left) movement at storm date March 28, 2012, 17:10 hours. Where the point black is the centroid at initial time and the red point is the centroid at the final time. In some cases there is more than one centroid and it can present more than one black and red point. This happens when the division cloud method occurs.

The current radar reflectivity is a function of the previous reflectivity images observed in surrounding areas centered on the location of a predicted pixel, and also is a function of the ratio of reflectivity of a pixel to reflectivity of the cell convective core.

The second postulated rainfall nowcasting algorithm task is predicting rainfall rate at each pixel.

1.11 Parameters Estimation

This methodology was applied to four (4) parameter unknowns $(\delta 1, \delta 2, \delta 3 \wedge \Phi)$ to find the optimum values with a bounded constraint, first linearized the main equation, second identify the initial point trough a nonlinear regression model where the phi Φ is temporarily ignored and the deltas values initial are obtained by solving the linear regression, third find the optimum values using a constrained nonlinear optimization

technique to estimate the final parameter set for each zone (9x9) and every window where the phi Φ parameter is a bias correction factor introduced in the optimization.

The optimum parameters for the nonlinear regression model were estimated by solving a constrained nonlinear optimization problem (*fmincon*).

Figure 4 -8 is the median of the value phi for lead-time 20 minutes.

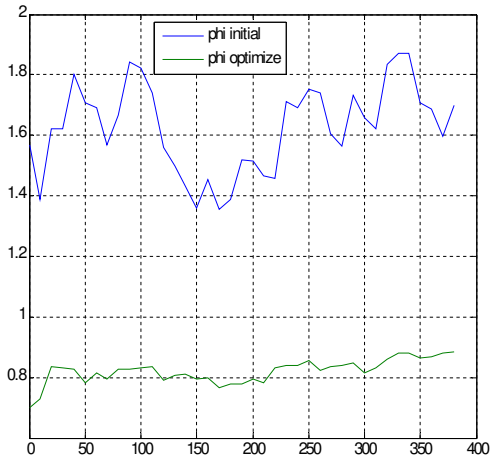

Figure 4-8. Phi median, storm date: March 28, 2012, lead-time of 20 min.

Figure 4 -9 presents the distribution of initial variable phi (Φ) and the optimal value for a lead-time of 30 minutes.

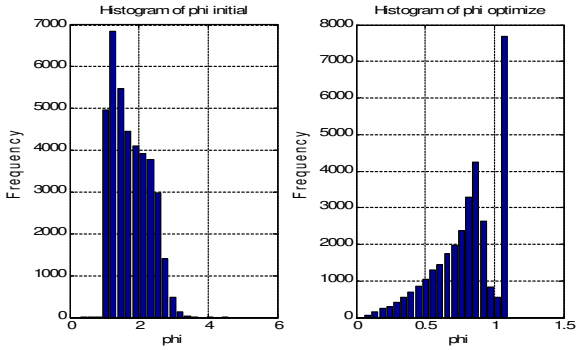

Figure 4-9. Distribution of initial value of phi (left) and the optimal values of phi (right) for the storm date: March 28, 2012,for a lead-time of 30 min.

Table 4-4. Detection results for ten storms with lead-time of 10 minutes.

Detection Results										
Skill Score	**Forecast**									
Dates	**20120328**	**20120329**	**20120430**	**20121010**	**20140212**	**20140629**	**20140705**	**20140506**	**20140630**	**20140521**
HR	0.8774111	0.963596	0.9141715	0.8068047	0.9003213	0.9487279	0.8455507	0.9385759	0.8697176	0.9141775
POD	0.7123848	0.6272294	0.6391765	0.63715	0.5290473	0.6197455	0.6070954	0.4439358	0.6297536	0.5509015
FAR	0.2068765	0.3348994	0.294561	0.2857665	0.3400653	0.3121831	0.2686225	0.3931983	0.212944	0.3158428
Detection Bias	0.8982017	0.9430594	0.9060692	0.8920752	0.8016661	0.9010326	0.8300713	0.7315994	0.8001382	0.8052266
PI	0.7943065	0.7519754	0.752929	0.7193961	0.6964345	0.7520967	0.7280079	0.6631045	0.7621758	0.716412

Table 4-5. Detection results for ten storms with lead-time of 20 minutes.

Detection Results										
Skill Score	**Forecast**									
Dates	**20120328**	**20120329**	**20120430**	**20121010**	**20140212**	**20140629**	**20140705**	**20140506**	**20140630**	**20140521**
HR	0.829492	0.9586175	0.8965384	0.7430307	0.8648185	0.9154759	0.7814875	0.9160943	0.8124894	0.8905689
POD	0.6080734	0.4684846	0.5183947	0.5362466	0.3889142	0.4556096	0.5024324	0.2493413	0.5423473	0.4380003
FAR	0.2816578	0.4893022	0.4345089	0.3649257	0.4751152	0.465673	0.4089899	0.6057553	0.3278306	0.4179181
Detection	0.846495	0.917342	0.916715	0.844384	0.740951	0.852679	0.850124	0.632453	0.806861	0.752472

Bias	5	2	9	1	6	3	8	2	1	1
PI	0.7186359	0.6459333	0.6601414	0.6381172	0.5928725	0.6351375	0.6249767	0.5198934	0.6756687	0.6368837

5 CHAPTER - CONCLUSION

Here you summarize all the important contributions of your work. Bla blab la
The rms difference between modeled and measured TB was reduced by 32%, from 1.56 K to 1.06 K, with the new parameters. Sensitivity analysis shows that the standard deviations on the CL, CW, CX parameters are 5% or less, and 8% for CC assuming 0.5K noise in the TB data. Correlation analysis between coefficients shows a high correlation between the errors in oxygen and the continuum terms.

The rms difference between modeled and measured TB was reduced by 32%, from 1.56 K to 1.06 K, with the new parameters. Sensitivity analysis shows that the standard deviations on the CL, CW, CX parameters are 5% or less, and 8% for CC assuming 0.5K noise in the TB data. Correlation analysis between coefficients shows a high correlation between the errors in oxygen and the continuum terms. Bla bla bla

REFERENCES

Anderson, T.W and D.A. Darling, [1954]. "A Test of Goodness-of-Fit." *Journal of the American Statistical Association* 49: 765–769.

Allen, R. G., L. S. Pereira, Dirk Raes and M. Smith, [1998]. *Crop Evapotranspiration Guidelines for Computing Crop Water Requirements*. FAO Irrigation and Drainage Paper 56, Food and Agriculture Organization of the United Nations,

Ball, J.E., and K.C. Luk, [1998]. "Modeling the spatial variability of rainfall over a catchment." ASCE, *Journal of Hydrologic Engineering*, 3[2]:122-130. DOI 10.1061/(ASCE)1084-0699(1998)3:2(122)

Battan, L.J., (1973). *Radar observation of the atmosphere*. University of Chicago Press, 323 pp.

Bear, J., (1972). *Dynamics of Fluids in Porous Materials*. American Elsevier, 784 pp.

Entekahbi, D., M.P. Anderson, R. Avissar, R. Bales, G.M. Hornberger, W.K. Nuttle, M.B. Parlange, C. Peters-Lidard, K.W. Potter, J.O. Roads, J.L. Wilson, and E.F. Wood, (2002). *Report of a Workshop on Predictability and Limits to prediction in Hydrologic Systems.* Committee on Hydrologic Science, National Research Council, National Academy Press, ISBN 0-309-08347-8. pp. 118.

FEMA, (2009*). Flood Insurance Study*. Commonwealth of Puerto Rico, Volume 1 of 5,

Georgakakos, K.P., (2006b). "Hydrologic Short Term Forecasting with QPF Input." White *Paper in Proceedings of USWRP Warm Season Precipitation Workshop*, 5-7 March 2002, National Center for Atmospheric Research, Boulder, Colorado, 5 pp.

Gourley, J. J. and B.E. Vieux, (2005). "A method for evaluating the accuracy of quantitative precipitation estimates from a hydrologic modeling perspective." *American Meteorological Society*. April, 115-133.

Hydrologic Engineering Center, (2008). *HEC-RAS River Analysis System*. Version 4.0 U.S. Army Corps of Eng, Davis, CA.

Minitab Inc, (2010). "Meet MINITAB 16 for Windows®." English Version. www.minitab.com

NOAA, (2006). *Puerto Rico Mean Annual Precipitation 1971-2000*. Hydrology and River Information. National Oceanic and Atmospheric Administration, National Weather Service ForecastOffice, San Juan, Puerto Rico, URL:http://www.srh.noaa.gov/sju/?n=mean_annual_precipitation

NOAA, (No date). Advanced Hydrologic Prediction Service (Online). Available: http://water.weather.gov/ahps2/hydrograph.php?wfo=sju&gage=horp4

Rawls, W.J., Brakensiek, D.L., Miller, N., (1983). "Green-Ampt Infiltration Parameters from Soils Data." *Journal of Hydraulic Engineering* 109(1), 62 – 70.

Rojas-González, A.M., (2004). "Estudio Comparativo sobre hidráulica de ríos en valles aluviales", Master of Science Thesis, University of Puerto Rico at Mayagüez , PR., 140 pp.

Sun, X., Mein, R.G., Keenan, T.D., Elliott, J.F., 2000. Flood estimation using radar and raingauge data. *Journal of Hydrology* 239 (1–4), 4–18.

Tarboton, D.G., R.L. Bras, and I. Rodriguez-Iturbe, (1991). "On extraction of channel networks from digital elevation data." *Hydrolog. Process*., 5, 81-100.

U.S. Census Bureau, (2010). Census 2010 Data for Puerto Rico. U.S. Census Bureau.

USACE, (1996). *Hydrologic Aspects of Flood Warning Preparedness Programs*.

U.S. Department of Agriculture, Natural Resources Conservation Service, (2006c). *Soil Survey Geographic (SSURGO) database for Arecibo area*. Puerto Rico Western Part, pr682, Fort Worth, Texas, Publication date: Dec. 26. URL:http://SoilDataMart.nrcs.usda.gov/

Van der Perk, M. and M.F.P. Bierkens, (1997). "The identifiability of parameters in a water quality model of the Biebzra river, Poland." *Journal of Hydrology* 200, 307-322.

Vieux, B.E., V.F. Bralts, Segerlind and R.B. Wallace, (1990). "Finite element watershed modeling: one-dimensional elements." *J. Water Resour. Plan. Mgmt* 116(6):803–819.